The EMBO Journal (2013) 32, 424–436
www.embojournal.org

TRANSPARENT PROCESS

THE EMBO JOURNAL

CENP-T provides a structural platform for outer kinetochore assembly

Since Advance Online Publication, two names have been added to the Acknowledgements

Tatsuya Nishino[1], Florencia Rago[2], Tetsuya Hori[1], Kentaro Tomii[3], Iain M Cheeseman[2] and Tatsuo Fukagawa[1,*]

[1]Department of Molecular Genetics, National Institute of Genetics and The Graduate University for Advanced Studies (SOKENDAI), Shizuoka, Japan, [2]Whitehead Institute for Biomedical Research and Department of Biology, Massachusetts Institute of Technology, Cambridge, MA, USA and [3]Computational Biology Research Center, National Institute of Advanced Industrial Science and Technology, Tokyo, Japan

The kinetochore forms a dynamic interface with microtubules from the mitotic spindle during mitosis. The Ndc80 complex acts as the key microtubule-binding complex at kinetochores. However, it is unclear how the Ndc80 complex associates with the inner kinetochore proteins that assemble upon centromeric chromatin. Here, based on a high-resolution structural analysis, we demonstrate that the N-terminal region of vertebrate CENP-T interacts with the 'RWD' domain in the Spc24/25 portion of the Ndc80 complex. Phosphorylation of CENP-T strengthens a cryptic hydrophobic interaction between CENP-T and Spc25 resulting in a phospho-regulated interaction that occurs without direct recognition of the phosphorylated residue. The Ndc80 complex interacts with both CENP-T and the Mis12 complex, but we find that these interactions are mutually exclusive, supporting a model in which two distinct pathways target the Ndc80 complex to kinetochores. Our results provide a model for how the multiple protein complexes at kinetochores associate in a phospho-regulated manner.

The EMBO Journal (2013) **32,** 424–436. doi:10.1038/emboj.2012.348; Published online 18 January 2013
Subject Categories: cell cycle
Keywords: CENP-T; kinetochore; mitosis; Spc24/25; X-ray structure

Introduction

The kinetochore forms a dynamic interface with microtubules from the mitotic spindle to facilitate faithful chromosome segregation during mitosis (Cheeseman and Desai, 2008; Santaguida and Musacchio, 2009). To establish a functional kinetochore, two key groups of structural proteins are required. First, a subset of inner kinetochore proteins binds to centromeric DNA to provide a platform for kinetochore assembly. Second, additional outer kinetochore proteins are recruited to centromeres to form robust interactions with spindle microtubules. The kinetochore-microtubule interface is composed of the highly conserved kinetochore complexes referred to as the KMN network, which includes *K*NL1, the four subunit *M*is12 complex (Mis12, Nnf1, Nsl1, and Dsn1), and the four subunit *N*dc80 complex (Ndc80, Nuf2, Spc24, and Spc25) (DeLuca and Musacchio, 2012). Depletion of any component of KMN proteins results in mitotic defects and a reduction in kinetochore-microtubule attachments (DeLuca *et al*, 2002; Martin-Lluesma *et al*, 2002; Hori *et al*, 2003; McCleland *et al*, 2003, 2004; Cheeseman *et al*, 2004, 2006, 2008; Obuse *et al*, 2004; DeLuca *et al*, 2006; Kline *et al*, 2006; Kiyomitsu *et al*, 2007). The KMN network binds directly to microtubules *in vitro* (Cheeseman *et al*, 2006; McIntosh *et al*, 2008; Powers *et al*, 2009). In particular, the Ndc80 complex has structural properties including an extended rod-shaped structure and a direct interaction with the microtubule lattice that make it well suited to act as the primary kinetochore-microtubule interface (Cheeseman *et al*, 2006; Wei *et al*, 2007; Ciferri *et al*, 2008; Wilson-Kubalek *et al*, 2008; Alushin *et al*, 2010). However, it is still unclear how the Ndc80 complex associates with inner kinetochore proteins to target this key complex to centromeres.

In contrast to the outer kinetochore, which is required only during mitosis, inner kinetochore components localize to centromeres throughout the cell cycle. This constitutive centromere-associated network of proteins (CCAN) (Okada *et al*, 2006; Cheeseman and Desai, 2008; Hori *et al*, 2008; Amano *et al*, 2009; Perpelescu and Fukagawa, 2011) provides a platform for outer kinetochore assembly. For example, the CCAN component CENP-C directly associates with the Mis12 complex (Liu *et al*, 2006; Kwon *et al*, 2007; Gascoigne *et al*, 2011; Przewloka *et al*, 2011; Screpanti *et al*, 2011). In addition, we have previously found that the CCAN component CENP-T is required to recruit the KMN network and assemble functional kinetochores (Hori *et al*, 2008; Gascoigne *et al*, 2011; Suzuki *et al*, 2011). CENP-T is an extended molecule that spans the inner and outer kinetochore (Suzuki *et al*, 2011). The C-terminal region of CENP-T forms a complex with the histone-fold containing proteins CENP-W, CENP-S, and CENP-X to form a nucleosome-like structure that binds to centromeric DNA (Hori *et al*, 2008; Nishino *et al*, 2012). The N-terminal region of CENP-T associates with the outer kinetochore and is sufficient to direct aspects of outer kinetochore assembly, including binding to and recruitment of the Ndc80 complex in a manner that depends upon the phosphorylation of CENP-T by cyclin-dependent kinase (CDK) (Gascoigne *et al*, 2011). Based on structural predictions, the N-terminal region of CENP-T lacks a defined structure and it is unclear how it associates with the Ndc80 complex. In addition,

*Corresponding author. Department of Molecular Genetics, National Institute of Genetics, Mishima, Shizuoka 411-8540, Japan.
Tel.: +81 55 981 6792, Fax: +81 55 981 6742,
E-mail: tfukagaw@lab.nig.ac.jp

Received: 1 August 2012; accepted: 14 December 2012; published online: 18 January 2013; corrected: 6 February 2013

the basis for the phospho-regulated interaction between CENP-T and the Ndc80 complex is unknown.

To define the nature of the link between the inner and outer kinetochore, we analysed the structural, biochemical, and functional basis for the CENP-T–Ndc80 complex interaction. We found that phosphorylated and phospho-mimetic peptides from the N-terminal region of CENP-T interact with the Spc24/Spc25 portion of the Ndc80 complex. Multiple kinetochore proteins, including Spc24/25, contain 'RWD' domains that are also found in functionally diverse proteins including RING finger proteins, WD-repeat containing proteins, and DEXD-like helicases (Schmitzberger and Harrison, 2012). It has been proposed that RWD domains provide interaction platforms to mediate kinetochore assembly. However, it is unclear how other proteins associate with these domains. Our high-resolution structure of the phospho-CENP-T–Spc24/25 complex reveals that the phosphorylated residues in CENP-T are not directly involved in the interaction with Spc25, but instead form a salt bridge to allow adjacent downstream hydrophobic residues to interact with the RWD containing Spc24/25 complex. Our results provide a model for how the multiple protein complexes at kinetochores associate in a phospho-regulated manner.

Results

The N-terminal region of CENP-T is critical for outer kinetochore assembly

We have shown previously that the N-terminal region of CENP-T is essential for kinetochore assembly in both human and chicken cells (Gascoigne *et al*, 2011). In particular, we found that the N-terminal 100 amino acids of CENP-T are phosphorylated by CDK to regulate outer kinetochore assembly. To define which regions of CENP-T are critical for recruiting downstream proteins, we tested several deletion constructs within this region (Δ1–30, Δ1–60, Δ69–90, and Δ1–90) using a complementation assay in CENP-T-deficient chicken DT40 cells (Figure 1A). Whereas CENP-T-deficient cells expressing either Δ1–30 or Δ1–60 grew similarly to control cells, CENP-T Δ1–90 and Δ69–90 could not rescue CENP-T depletion (Figure 1A and B). This suggests that an ∼20 aa sequence near the N-terminal region of CENP-T that includes the CDK phosphorylation sites T72 and S88 is critical for CENP-T function. Indeed, we found that Ndc80 localization to kinetochores was reduced in cells expressing only CENP-T Δ69–90 or Δ1–90 (Figure 1C; data not shown). Interestingly, an in frame fusion between Spc25 and CENP-T Δ1–90 recruited Ndc80 to kinetochores (Figure 1D) and partially rescued the loss of viability resulting from the depletion of endogenous CENP-T (Figure 1E). This suggests that a primary function for the CENP-T N-terminal region is to interact with the Ndc80 complex and direct outer kinetochore assembly.

The CENP-T N-terminal region displays phospho-dependent binding to the Spc24/25 complex

We next sought to define the specific interactions between the N-terminal region of CENP-T and outer kinetochore components. We have shown previously that recombinant human CENP-T-W complex binds directly to the engineered Ndc80^{Bonsai} complex (Gascoigne *et al*, 2011). The Ndc80 complex has two globular regions separated by an extended coiled-coil with the Ndc80/Nuf2 portion binding to microtubules (Cheeseman *et al*, 2006; Wei *et al*, 2007; Ciferri *et al*, 2008; Wilson-Kubalek *et al*, 2008; Alushin *et al*, 2010) and the Spc24/25 portion facing the inner kinetochore (DeLuca *et al*, 2006; Wei *et al*, 2006). To determine whether the CENP-T N-terminal region can interact directly with the Spc24/25 portion of the Ndc80 complex, we analysed the binding between the globular regions of the chicken Spc24/25 sub-complex (125–195 aa of chicken Spc24 and 132–234 aa of chicken Spc25) and chicken CENP-T fragments *in vitro*. For these experiments, we used both unmodified and phospho-mimetic CENP-T (T72D and S88D) as a Maltose Binding Protein (MBP) fusion. Based on the shift in migration for the Spc24/25 sub-complex as assessed by size-exclusion chromatography, the phospho-mimetic CENP-T N-terminal region (using either amino acids 2–98 or 63–98) binds efficiently to Spc24/25 (Figure 2A; Supplementary Figure S1). In contrast, either fragment of unphosphorylated wild-type CENP-T or phospho-deficient CENP-T (T72A and S88A) did not bind as strongly to the Spc24/25 complex (Figure 2B; Supplementary Figure S1). In addition, although CENP-T fragments containing the extreme N-terminal region of CENP-T (chicken aa 2–50 or human aa 2–32) also have CDK phosphorylation sites, these fragments did not show detectable interactions with the Spc24/25 complex (Supplementary Figure S1).

As we found that both short (63–98) and long (2–98) peptides of CENP-T bound to the Spc24/25 complex (Figure 2A; Supplementary Figure S1), we next determined K_D's for this binding using composition gradient multi-angle light scattering (CG-MALS) and isothermal titration calorimetry (ITC) (Figure 2C–H). Based on ITC measurements, the K_D for binding of the wild-type chicken CENP-T peptide to the chicken Spc24/25 complex was 6.67 μM (Figure 2F). Due to this weaker interaction, it was not possible to define a precise K_D for this interaction by CG-MALS. In contrast, phospho-mimetic and synthetic phosphorylated CENP-T peptides bound to more strongly to the Spc24/25 complex and formed a 1:1 stoichiometric complex. The doubly phospho-mimetic CENP-T (T72D and S88D) peptide bound to Spc24/25 with a K_D of 381 nM as measured by CG-MALS and 481 nM as measured by ITC (Figure 2C and D). Singly modified CENP-T (T72D) bound to the Spc24/25 complex with a K_D of 610 nM based on ITC (Figure 2E). Similarly, singly or doubly synthetic phosphorylated CENP-T peptides (either a T72p/S88p double phospho-peptide or a T72p single phospho-peptide) bound to the Spc24/25 complex with K_D's of 518 nM or 1.29 μM, respectively, based on ITC measurements (Figure 2G and H). As doubly phosphorylated or phospho-mimetic CENP-T showed increased binding to Spc24/25 relative to singly phosphorylated CENP-T, we used the T72D and S88D double mutant for all subsequent assays.

We have previously shown that unphosphorylated human CENP-T-W binds to the engineered human Ndc80^{Bonsai} complex (Gascoigne *et al*, 2011). Unlike chicken CENP-T, the unphosphorylated human CENP-T N-terminal fragment (amino acids 76–106) fused with MBP bound to the human Spc24/25 (137–197 aa of human Spc24 and 129–224 aa of human Spc25) complex with a K_D of 645 nM based on ITC (Supplementary Figure S1) and to the Ndc80^{Bonsai} complex based on gel filtration (Supplementary Figure S2A). We also confirmed that the unphosphorylated human CENP-T N-terminal region (1–375 aa) without the MBP fusion

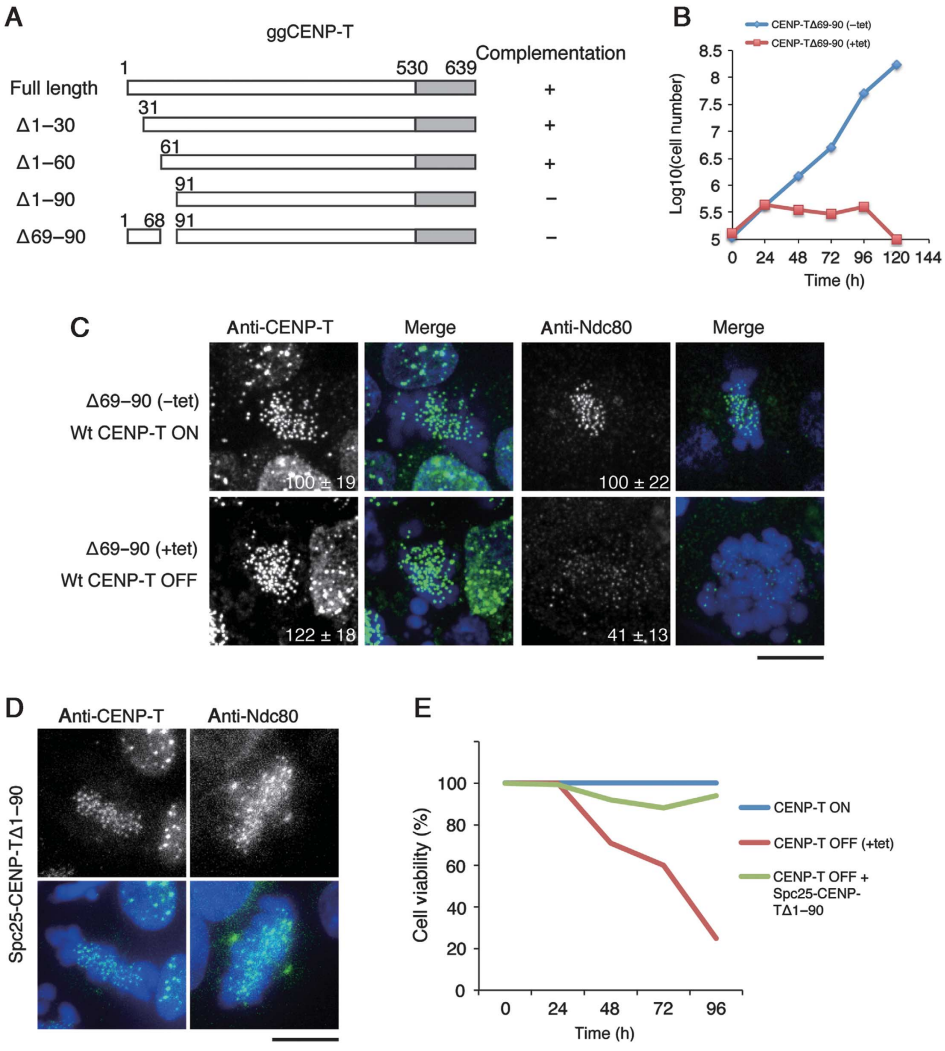

Figure 1 The CENP-T N-terminal region is required for kinetochore localization of the Ndc80 complex. (**A**) Diagram showing the chicken CENP-T sequence and the tested deletion mutants in the CENP-T N-terminal region. '+' or '−' indicates whether the given deletion mutant can complement growth when endogenous CENP-T is depleted. (**B**) Graph showing the growth curve of cells expressing CENP-TΔ69–90 in the presence (red rectangle) or absence (blue diamond) of tetracycline to repress the expression of wild-type CENP-T. (**C**) Immunofluorescence analysis of cells expressing CENP-T Δ69–90 after 72 h in the presence (lower panel) or absence (upper panel) of tetracycline to repress the expression of wild-type CENP-T. Cells were probed for either CENP-T or Ndc80 and the kinetochore signal intensities of each protein were measured relative to an adjacent background signal. Bar, 10 μm. (**D**) Immunofluorescence analysis of cells in which expression of CENP-T is replaced with a Spc25-Δ1–90-CENP-T fusion protein. Ndc80 localizes to kinetochores in these cells, unlike the CENP-T Δ69–90 mutant alone in (**C**). (**E**) Cell viability analysis for CENP-T conditional knockout cells in the presence (CENP-T OFF) or absence (CENP-T ON) of tetracycline, or expressing a Spc25-Δ1–90 CENP-T fusion protein in the presence of tetracycline (CENP-T OFF + Spc25-Δ1–90 CENP-T).

Figure 2 Phospho-mimetic CENP-T binds directly to the Spc24/25 portion of the Ndc80 complex. (**A**) Top, traces (OD_{214}) from the gel filtration column showing the co-migration of chicken $Spc24^{125–195}/Spc25^{132–234}$ with phospho-mimetic chicken CENP-T (63–98; T72D and S88D). The phospho-mimetic CENP-T fused with MBP and the globular domains of the Spc24/25 complex were tested individually or mixed and incubated for 15 min at room temperature prior to separation by gel filtration using a Superdex 75 column. Bottom, peak fractions were analysed by SDS–PAGE and stained with Coomassie. (**B**) Non-phosphomimetic $CENP\text{-}T^{63–98}$ does not strongly interact with Spc24/25. Wild-type $MBP\text{-}CENP\text{-}T^{63–98}$ and the $Spc24^{125–195}/Spc25^{132–234}$ complex were analysed as in (**A**). (**C**) The phospho-mimetic chicken CENP-T N-terminal region binds to Spc24/25 with high affinity. Composition gradient multi-angle light scattering (CG-MALS) analysis of phospho-mimetic $MBP\text{-}CENP\text{-}T^{63–98}$ together with the globular domain of the $Spc24^{125–195}/Spc25^{132–234}$ complex. Nine different composition gradients were analysed by multi-angle light scattering to measure the molar mass. Composition of various forms of proteins was calculated by fitting the CG-MALS data and the concentration distribution graph is shown. The two components interacted with 1:1 stoichiometry with a K_D of 381 nM. (**D**) ITC binding curve for the interaction of phospho-mimetic chicken $CENP\text{-}T\ peptide^{63–98}$ (T72D and S88D) with the $Spc24^{125–195}/Spc25^{132–234}$ complex. The measured K_D is 481 nM. (**E**) ITC binding curve for the interaction of singly phospho-mimetic chicken $CENP\text{-}T\ peptide^{63–98}$ (T72D) with the $Spc24^{125–195}/Spc25^{132–234}$ complex. The measured K_D is 610 nM. (**F**) ITC binding curve for the interaction of wild-type chicken $CENP\text{-}T\ peptide^{63–98}$ with the $Spc24^{125–195}/Spc25^{132–234}$ complex. The measured K_D is 6.67 μM. (**G**) ITC binding curve for the interaction of a synthetic phosphorylated chicken $CENP\text{-}T\ peptide^{63–98}$ (T72p and S88p) with the $Spc24^{125–195}/Spc25^{132–234}$ complex. The measured K_D is 518 nM. (**H**) ITC binding curve for the interaction of a synthetic phosphorylated chicken $CENP\text{-}T\ peptide^{63–98}$ (T72p) with the $Spc24^{125–195}/Spc25^{132–234}$ complex. The measured K_D is 1.29 μM.

bound to the Ndc80^{Bonsai} complex by gel filtration (Supplementary Figure S2B). However, phospho-mimetic human CENP-T showed increased binding to the Ndc80^{Bonsai} complex based on gel filtration (Supplementary Figure S2A and B) and bound to the human Spc24$^{131–197}$/Spc25$^{129–224}$ complex with a K_D of 150 nM by ITC (Supplementary Figure S1). Based on the combination of these biochemical data, we conclude that the phosphorylated human or chicken CENP-T N-terminal region directly associates with the Spc24/25 portion of the Ndc80 complex.

The CENP-T N-terminal region binds to the Spc24/25 complex through hydrophobic and electrostatic interactions

The Spc24/25 complex contains two 'RWD' domains, which are found in multiple proteins and are thought to provide a

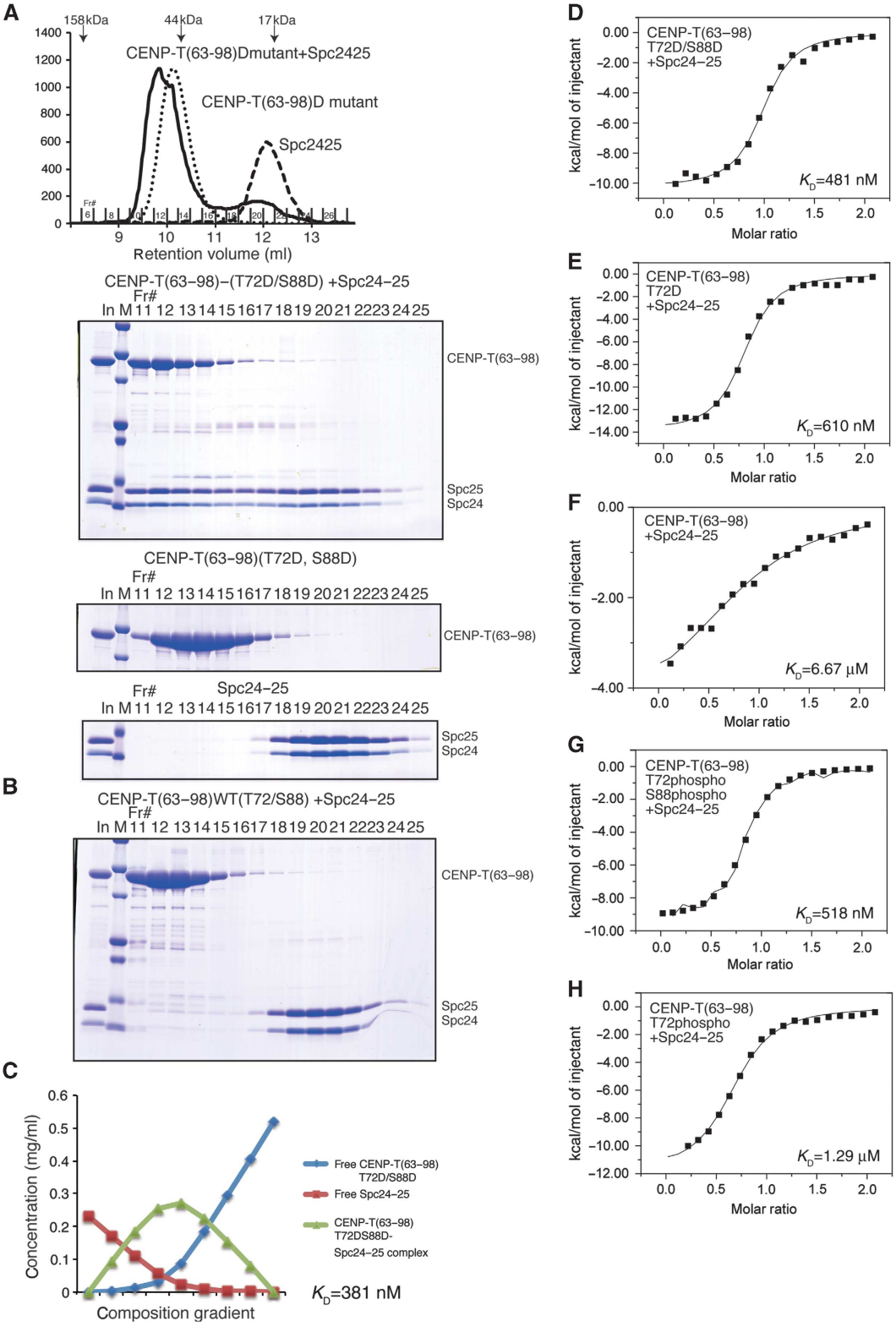

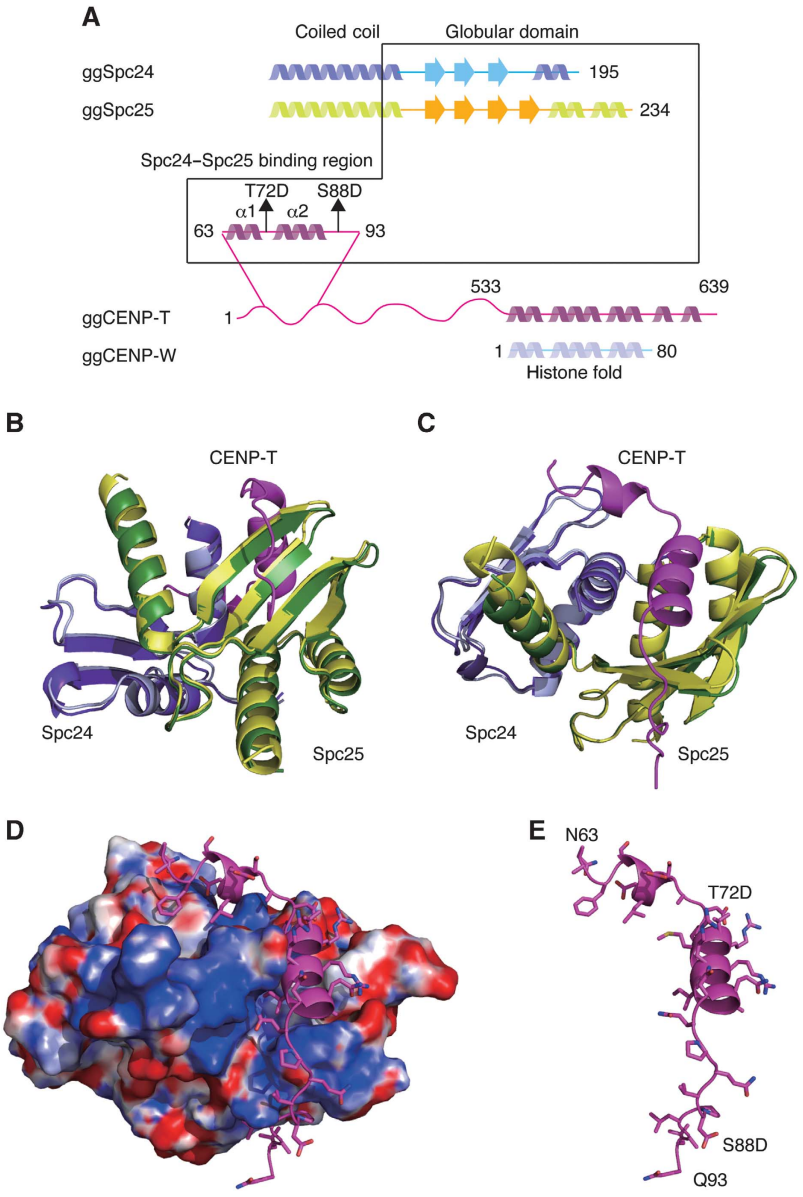

Figure 3 Crystal structure of the phospho-mimetic CENP-T–Spc24/25 complex. (**A**) Schematic diagram of Spc24, Spc25, CENP-T, and CENP-W showing the presence of α-helices and β-sheets. The expression constructs used for the structural analyses are indicated by the box. (**B**) Structural model showing the side view of the Spc24/25 complex superimposed with the CENP-T–Spc24/25 complex. For the Spc24/25 complex, Spc24 is coloured in light cyan and Spc25 is in light green. For the CENP-T–Spc24/25 complex, CENP-T is coloured in magenta, Spc24 is cyan, and Spc25 is green. (**C**) Structural model showing the top view of the superimposed structures of the Spc24/25 complex and the CENP-T–Spc24/25 complex as in (**B**). (**D**) Structural model showing the surface charge of the Spc24/25 complex interacting with phospho-mimetic CENP-T peptide. Electrostatic surface charges of the Spc24/25 complex were calculated by APBS and are contoured from −8.0 (red) to 8.0 (blue). The complex is viewed from the same angle as in (**C**). Side chains of CENP-T are shown as stick models. (**E**) Structural model showing the phospho-mimetic CENP-T peptide from the CENP-T–Spc24/25 complex structure in (**D**) on its own.

platform for protein–protein interactions (Schmitzberger and Harrison, 2012). To define the mechanisms by which the phosphorylated CENP-T N-terminal region binds to the RWD-containing Spc24/25, we conducted a high-resolution structural analysis of phospho-mimetic chicken CENP-T (63–98 aa) together with the globular regions of recombinant Spc24 and Spc25 (125–195 aa of chicken Spc24 and 132–234 aa of chicken Spc25) (Figure 3A). We also determined the structure of the Spc24/25 complex alone. Following crystallization of these protein complexes, we determined their structures by molecular replacement methods with a model based on the engineered human Ndc80^{Bonsai} complex (Ciferri *et al*, 2008) (Figure 3B–E; Table I). The chicken Spc24/25 complex was refined to 1.0 Å resolution with refinement statistics of $R_{work} = 0.193$ ($R_{free} = 0.207$) and the CENP-T-Spc24/25 complex was refined to 1.9 Å resolution with refinement statistics of $R_{work} = 0.167$ ($R_{free} = 0.216$). We superimposed each structural model and confirmed that the structures of the Spc24/25 sub-complex from each model were identical (Figure 3B and C). The CENP-T peptide (63–98 aa) contains two α-helices (Figure 3B–E; Supplementary Figure S3) with the second helical region closely associated with a β-sheet from Spc25 (Figures 3 and 4A). An extended coil follows the CENP-T helices and there are additional

Table I X-ray diffraction data and model refinement statistics for the Sps24/25 complex and CENP-T$^{63-98}$T72DS88D–Spc24/25 complex

	Spc24–Spc25 globular domain	CENP-T(63–98)T72DS88D Spc24–Spc25 globular domain
Data collection		
Space group	P212121	$P3_1$
Unit-cell parameters (Å)	$a = 47.21$, $b = 58.08$ Å, $c = 58.41$ Å, $\alpha = \beta = \gamma = 90^\circ$	$a = b = 61.32$ Å, $c = 111.28$ Å, $\alpha = \beta = 90^\circ$, $\gamma = 120^\circ$
Wavelength (Å)	1	1
Resolution (Å)	1.03	1.9
Completeness (%)[a]	99.2 (100)	99.9 (99.9)
f'/f''		
$R_{mrgd\text{-}F}$ (%)[a]	4.3 (30.5)	6.0 (53.6)
$I/\sigma(I)$[a]	49.0 (5.25)	30.4 (3.55)
Number of reflections	79 657	36 934
Refinement statistics		
Resolution range (Å)	41.2–1.03	30.41–1.90
R_{work}/R_{free} (%)[a]	19.3 (25.2)/20.7(24.4)	16.7(22.1)/21.6(23.4)
Number of atoms (mean B value)		
Protein	1366 (9.9)	3175 (26.1)
Water	251 (37.0)	357 (45.7)
R.m.s. deviations		
Bond length (Å)	0.006	0.022
Bond angle (deg)	1.092	1.92
Ramachandran plot (%)	98.7/1.3/0.0	98.7/1.3/0.0

[a]Number in parenthesis are values from highest resolution shell.

hydrophobic and electrostatic interactions with the β sheets from Spc25 (Figures 3 and 4A). In addition to this interaction between CENP-T and Spc25, we also found a second potential contact site for CENP-T with the Spc24 portion of the Spc24/25 complex. This interaction involves the first helix of the CENP-T peptide including the L68 residue (Figure 4A).

As the Spc24/25 complex shows increased binding to the phospho-mimetic CENP-T peptide relative to unphosphorylated CENP-T (Figure 2), we examined how the phospho-mimetic residues are involved in the interaction with the Spc24/25 complex. We found that this interaction is not electrostatic and that instead a hydrophobic interface from CENP-T contributes to this interaction to bind to Spc25 directly (Figure 4A). Therefore, T72D and S88D in CENP-T are not direct contact sites for the CENP-T–Spc25 interaction. Thus, we hypothesized that the T72D residue forms a salt bridge with R74 to allow the subsequent hydrophobic residues to orient towards the hydrophobic residues in Spc25 (Figure 4B). To test this, we generated R74 mutants (R74E or R74A) in phospho-mimetic CENP-T (T72D and S88D) to prevent the phospho-mimetic residue from forming a salt bridge between the 72 and 74 residues. As shown in Figure 4C, these CENP-T mutant peptides failed to interact with Spc24/25.

To test the role of the hydrophobic residues in mediating interactions between CENP-T and Spc24, we generated an L68R mutation in the context of the phospho-mimetic CENP-T peptide. The L68R mutant disrupted the CENP-T–Spc24/25 interaction even when the salt bridge between 72 and 74 was formed (Figure 4D). Based on our structural and mutational analysis, we conclude that phosphorylation of T72 facilitates formation of a salt bridge with R74 to allow the downstream hydrophobic residues in CENP-T to interact with the Spc24/25 complex. This interaction region of CENP-T, which contains T-P-R residues (72–74) and downstream hydrophobic residues, is well conserved in various eukaryotic species including *S. pombe* (Figure 4A; Supplementary Figure S3).

The binding of CENP-T and the Mis12 complex to the Spc24/25 is mutually exclusive

Based on our structural analysis of the CENP-T-Spc24/25 complex, we also predicted critical hydrophobic residues in the Spc24/25 complex (I156 and L161 in chicken Spc25 and I149 and L154 in human Spc25) that would be required for the CENP-T–Spc25 interaction. These residues are conserved between human and chicken Spc25 (Supplementary Figure S4). To test the role of these residues for the CENP-T–Spc24/25 interaction, we generated mutant Spc24/25 complexes containing chicken Spc25 (I156R) or Spc25 (L161R). These mutations did not affect complex formation with Spc24, but they failed to interact with the phospho-mimetic CENP-T peptide (Figure 5A and B). Similarly, phospho-mimetic human CENP-T showed reduced interactions with Ndc80^{Bonsai} complex containing a Spc25 mutant (I149A L154A) by gel filtration (Figure 5C). We also confirmed the reduced interactions of the Spc25 mutant with CENP-T using human Spc24/25 complex (57–197 aa of human Spc24 and 70–224 aa of human Spc25) based on gel filtration and ITC measurements (Supplementary Figure S5A and B). This suggests that these hydrophobic residues in Spc25 are directly involved in the interaction with vertebrate CENP-T.

Above we demonstrated that CENP-T interacts directly with the Spc24/25 sub-complex. However, the Ndc80 complex also associates with the Mis12 complex and KNL1 (Cheeseman *et al*, 2004; Obuse *et al*, 2004; Cheeseman *et al*, 2006; Maskell *et al*, 2010; Petrovic *et al*, 2010; DeLuca and Musacchio, 2012), and it was unclear whether the Ndc80

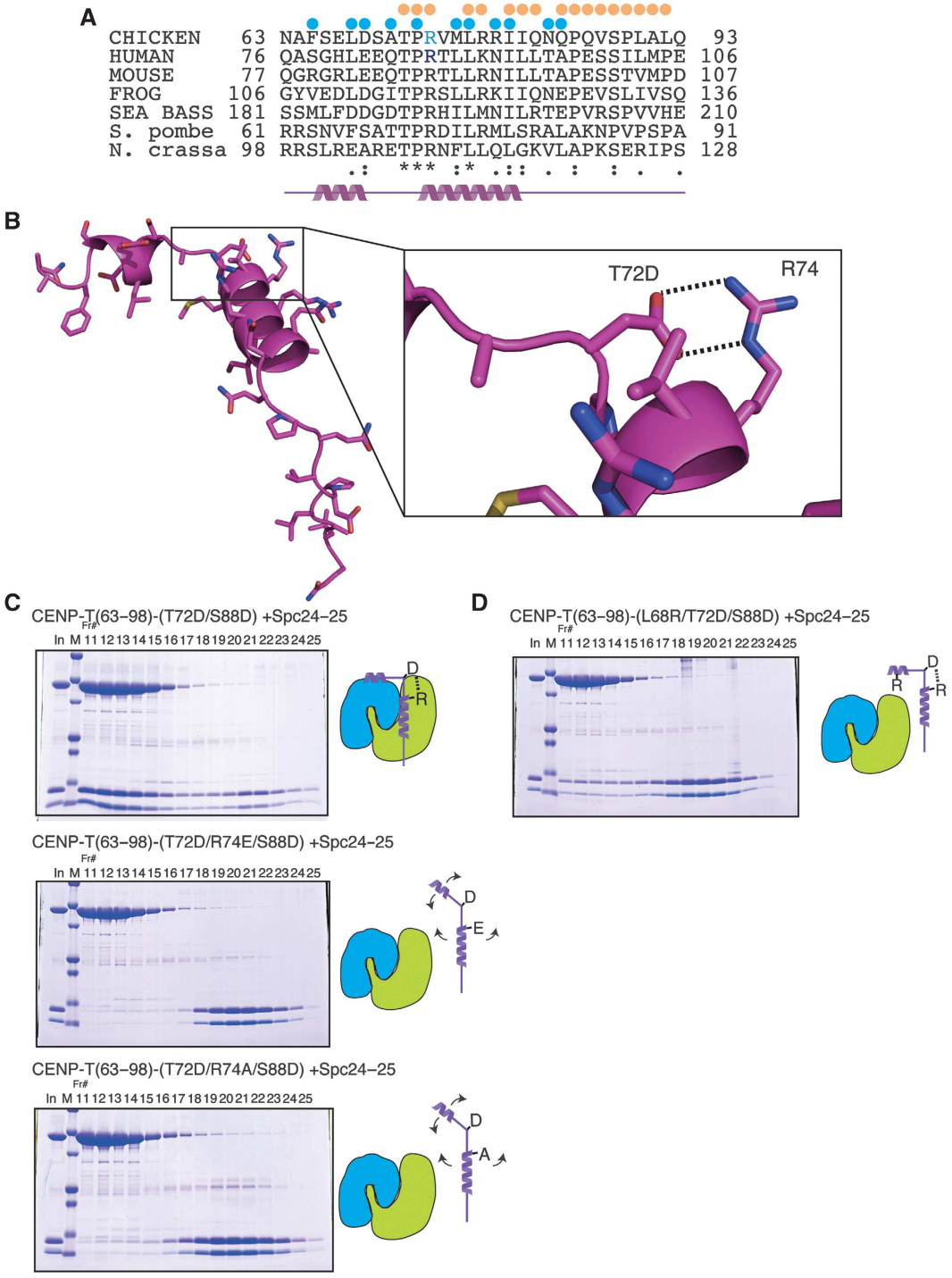

Figure 4 A conserved salt bridge is essential for the interaction of CENP-T with the Spc24/25 complex. (**A**) Sequence alignment of CENP-T from chicken, human, mouse, frog, sea bass, fission yeast, and filamentous fungi. Residues involved in the interaction of CENP-T with Spc24 and Spc25 are denoted by blue and orange dots, respectively. (**B**) Structural model showing a close-up view of the phospho-mimetic CENP-T peptide. The salt bridge between T72D and R74 is highlighted. (**C**) Mutation of CENP-T R74 (R74E or R74A) disrupts complex formation even in the presence of phospho-mimetic T72D and S88D residues. Stoichiometric amounts of MBP-CENP-T$^{63–98}$ mutant (T72D/R74E/S88D or T72D/R74A/S88D) and the Spc24$^{125-195}$/Spc25$^{132-234}$ complex were mixed and analysed by gel filtration as in Figure 2A. Upper panel: phospho-mimetic CENP-T (T72D/S88D) and the Spc24/25 complex interaction as in Figure 2A. Middle panel: CENP-T mutant (T72D/R74E/S88D) with the Spc24$^{125–195}$/Spc25$^{132–234}$ complex. Lower panel: CENP-T mutant (T72D/R74A/S88D) with the Spc24$^{125–195}$/Spc25$^{132–234}$ complex. Schematic diagrams of CENP-T and the Spc24/25 complex are shown to the right (blue: Spc24, green: Spc25). (**D**) CENP-T mutation at L68 disrupts complex formation with Spc24/25. Gel filtration analysis of the MBP-CENP-T$^{63–98}$ mutant (L68R7/T72D/S88D) with the Spc24$^{125–195}$/Spc25$^{132–234}$ complex as in (**C**).

complex can simultaneously interact with both CENP-T and Mis12/KNL1, or whether these represent mutually exclusive assembly pathways. The human Ndc80^{Bonsai} complex mutated for Spc25 (I149A L154A) displayed reduced binding to phospho-mimetic CENP-T (Figure 5C), but we found that the mutant Ndc80^{Bonsai} or the Spc24$^{57–197}$/Spc25$^{70–224}$ complex

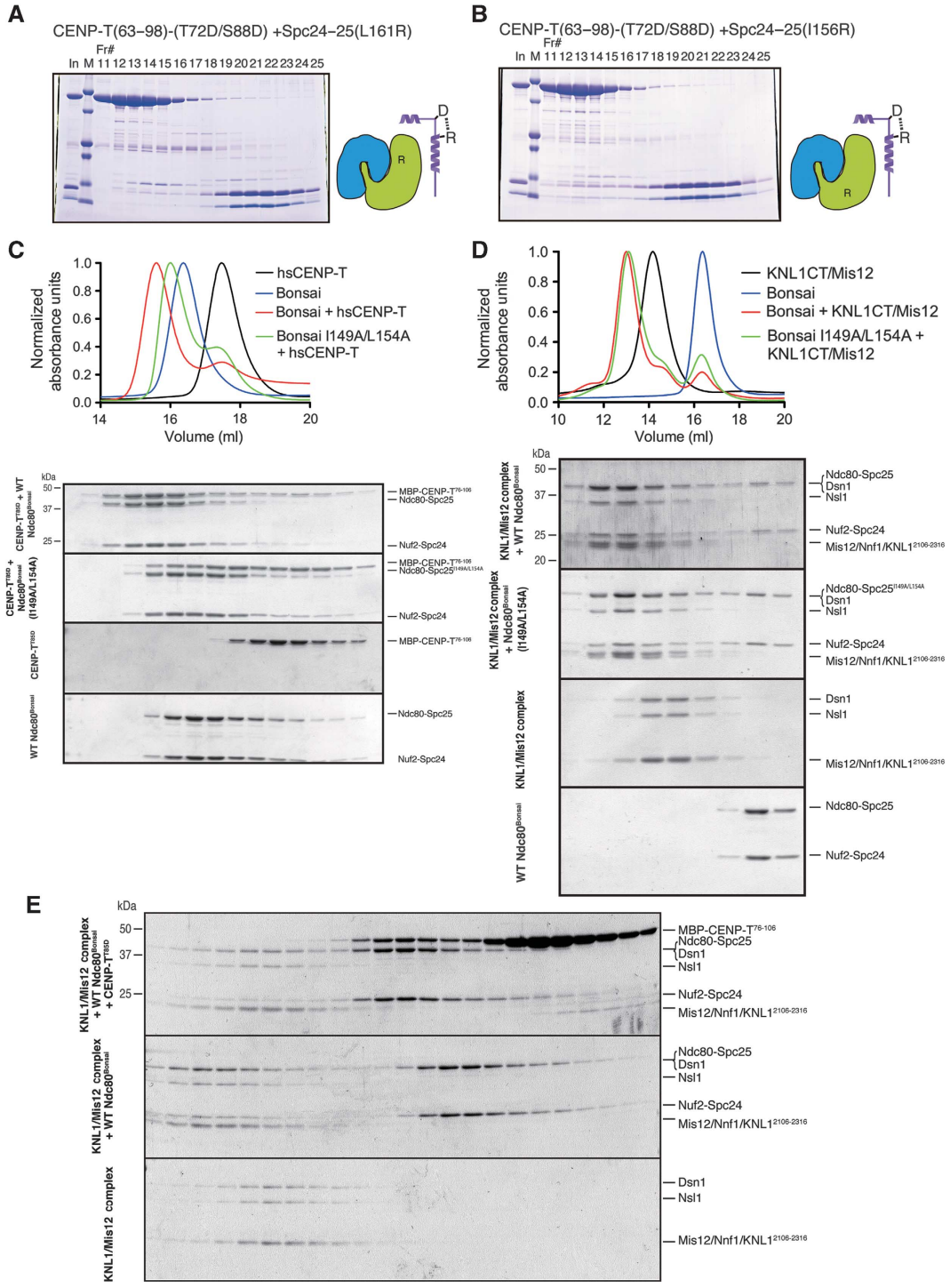

Figure 5 Binding of CENP-T and the Mis12 complex to the Ndc80 complex is mutually exclusive. (**A**) L161R mutations in Spc25 disrupt the interaction with CENP-T. Phospho-mimetic chicken MBP-CENP-T$^{63–98}$ (T72D/S88D) and the mutant Spc24$^{125–195}$/Spc25$^{132–234}$ (L161R) complex were separated by gel filtration using a Superdex 75, analysed by SDS–PAGE, and stained with Coomassie. (**B**) I156R mutations in Spc25 disrupt the interaction with CENP-T. Phospho-mimetic MBP-CENP-T$^{63–98}$ (T72D/S88D) and the mutant Spc24$^{125–195}$/Spc25$^{132–234}$ (I156R) complex were analysed by gel filtration as in (**A**). (**C**) I149A L154A double mutants in human Spc25 disrupt binding to human CENP-T. Human phospho-mimetic CENP-T (MBP-hsCENP-T$^{76–106}$ T85D) and the wild-type Ndc80^{Bonsai} complex or the Ndc80^{Bonsai} I149A L154A mutant complex were mixed and analysed by gel filtration. Protein mixtures were incubated on ice for 30 min before conducting the chromatography using a Superose 6 column. Fractions were collected, analysed by SDS–PAGE, and stained with Coomassie. Elution profiles from the size-exclusion chromatography for the experiment are shown (top). Elution of proteins was monitored at $A_{280\,nm}$. (**D**) The Ndc80^{Bonsai} complex or the Ndc80^{Bonsai} I149A L154A mutant complex and the human Mis12–KNL1$^{2106–2316}$ complex were mixed and analysed by gel filtration chromatography using a Superose 6 column as in (C). Elution profiles from the size-exclusion chromatography are shown (top). (**E**) CENP-T and the Mis12/KNL1^{CT} complex show mutually exclusive binding to the Ndc80^{Bonsai} complex. Human phospho-mimetic MBP-CENP-T$^{76–106}$(T85D), wild-type Ndc80^{Bonsai} complex, and the human Mis12-KNL1$^{2106–2316}$ complex were mixed in the indicated combinations and analysed by gel filtration. A large complex containing all components was not detected, although both CENP-T and KNL1/Mis12 bound individually to the Ndc80 complex based on altered migration.

still bound to the Mis12 complex based on gel filtration (Figure 5D; Supplementary Figure S5C). However, the binding affinity of the mutant Spc24$^{57-197}$/Spc25$^{70-224}$ complex for the Mis12 complex was reduced ($K_D = 291$ nM) compared with the wild-type Spc24$^{57-197}$/Spc25$^{70-224}$ complex ($K_D = 18.9$ nM) based on ITC measurements (Supplementary Figure S5D), suggesting that the binding sites of Spc24/25 for the Mis12 complex and CENP-T partially overlap.

Next, we tested whether the Ndc80^{Bonsai} complex could interact simultaneously with CENP-T and KNL1/Mis12 complex (Figure 5E). In separate experiments, we detected co-migration of the KNL1 and the Mis12 complex with the Ndc80^{Bonsai} complex and CENP-T with the Ndc80^{Bonsai} complex by gel filtration. However, co-migration of all proteins was not detected (Figure 5E; note lack of CENP-T in the largest fractions). Similar results were obtained with the Spc24$^{57-197}$/Spc25$^{70-224}$ complex (Supplementary Figure S5E). We have previously shown that the Mis12 complex bound weakly to CENP-T in pull-down assays (Gascoigne *et al*, 2011). In that case, we detected small amounts of Mis12 by western blot analysis. As we did not detect co-migration of the Mis12 complex with CENP-T (Figure 5E; Supplementary Figure S2C), this suggests that the Mis12 complex does not associate strongly with CENP-T. Based on these biochemical analyses, we conclude that the binding of the CENP-T N-terminal region and the Mis12 complex to the Spc24/25 is mutually exclusive likely due to competition for this interaction surface, as well as possibly steric exclusion.

The Ndc80 complex is recruited into kinetochores by two parallel pathways

We next sought to test the significance of the hydrophobic interaction of CENP-T with the Spc24/25 complex in cells. To do this, we generated a stable DT40 cell line expressing GFP-Spc25 (I156R) mutant and analysed the localization of this fusion protein. Wild-type Spc25 co-localized with CENP-T. In contrast, the localization of Spc25 (I156R) at kinetochores was reduced to ~60% of wild-type Spc25 (Figure 6A). To assess the functional consequences of the Spc25 mutant, we generated a conditional knock-out for Spc25 in DT40 cells (Supplementary Figure S6). Although DT40 cells in which expression of wild-type Spc25 was replaced with the Spc25 (I156R) mutant were viable, the growth rate of these cells was slightly reduced (Figure 6B). Based on these data, we conclude that the hydrophobic interaction of CENP-T with the Spc24/25 complex is required for the robust localization of the Spc24/25 complex to kinetochores.

We have previously shown that Ndc80 localization is greatly reduced in both CENP-T- and Mis12-deficient cells (Kline *et al*, 2006; Kwon *et al*, 2007; Gascoigne *et al*, 2011; Nishino *et al*, 2012). For these previous analyses, we conditionally repressed gene expression by addition of tetracycline such that protein levels were gradually reduced over several cell cycles. To evaluate the acute effects of CENP-T or Mis12 complex depletion on the localization of downstream factors, we used an auxin-based degron system (Nishimura *et al*, 2009) in which proteins are rapidly targeted for degradation. Using this system, we found that degradation of either CENP-T or the Mis12 complex subunit Dsn1 reduced the levels of Ndc80 at kinetochores by 43 or 32%,

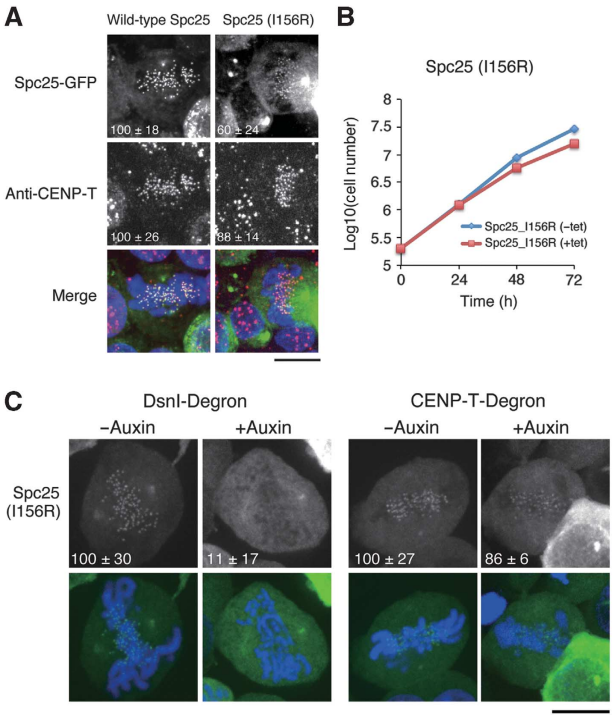

Figure 6 The Ndc80 complex is targeted to kinetochores by two parallel pathways. (**A**) Kinetochore localization of Spc25 I156R mutants was reduced to ~60% in DT40 cells. Immunofluorescence images showing the co-localization of chicken wild type or I156R mutant Spc25-GFP with CENP-T. Signal intensities of each protein were measured relative to an adjacent background signal. Bar, 10 μm. (**B**) Graph showing growth curves of DT40 cells in which expression of Spc25 is replaced with Spc25 I156R mutant. The doubling time of these cells was 14.2 h compared to 13.1 h for control cells. Tetracycline was added at time 0 to repress transcription of wild-type Spc25. (**C**) Spc25 mutants defective for CENP-T interactions require the Mis12 complex to localize to kinetochores. Images showing localization of Spc25 (I156R) in Dsn1- or CENP-T-degron cells. Dsn1 or CENP-T was degraded within 1 h after the addition of auxin (see Supplementary Figure S6).

respectively (Supplementary Figure S6). As Ndc80 localization was not abolished in either case, these data support a model in which there are two parallel pathways for targeting the Ndc80 complex to kinetochores. However, we note that CENP-T depletion also causes a reduction in Mis12 complex and KNL1 localization (Gascoigne *et al*, 2011). Therefore, we cannot exclude additional contacts with other regions of CENP-T that create an interrelationship between the Mis12 and CENP-T pathways.

Above, we found that the Spc25 (I156R) mutant failed to interact with CENP-T, but was still able to localize to kinetochores in DT40 cells (Figure 6A) suggesting that the Mis12 pathway for recruiting the Ndc80 complex is still active when the CENP-T–Spc25 interaction is compromised. Indeed, we found that Spc25 (I156R) localization to kinetochores was most completely abolished in Dsn1-degron cells, whereas weak Spc25 (I156R) signals were still visible in CENP-T-degron cells (Figure 6C). This result supports a model in which the Ndc80 complex is recruited by two-parallel pathways during mitosis and is consistent with biochemical analysis showing mutually exclusive interactions between CENP-T, the Ndc80 complex, and the Mis12 complex (Figure 5; Supplementary Figure S5).

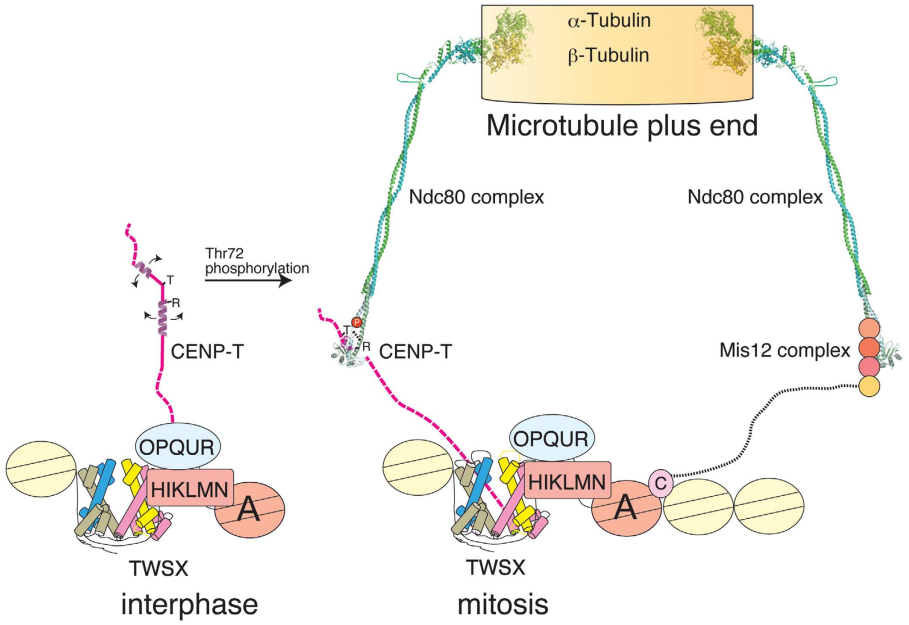

Figure 7 Parallel pathways for outer kinetochore assembly. Model for the molecular architecture of the kinetochore based on the structural, biochemical, and cell biological work presented in this paper. The CENP-T N-terminal region is unphosphorylated during interphase and phosphorylated by CDK during mitosis. The phosphorylated residue (T72 in chicken CENP-T) forms a salt bridge with R residues to allow adjacent downstream hydrophobic residues to interact with Spc24/25. The CENP-T pathway serves an important role to recruit the Ndc80 complex to kinetochores. In addition, a second parallel pathway for Ndc80 complex localization is mediated by the Mis12 complex.

Discussion

A major function for the kinetochore is to generate robust contacts with spindle microtubules to facilitate faithful chromosome segregation. The Ndc80 complex is a key kinetochore microtubule-binding component (Figure 7; Alushin *et al*, 2010). However, it was unclear how the Ndc80 complex is targeted to centromeric regions. Here, we demonstrated that the CENP-T N-terminal region binds directly to the Spc24/25 portion of the Ndc80 complex when CENP-T is phosphorylated to target the Ndc80 complex to kinetochores during mitosis. This interaction appears to be evolutionally conserved as the budding yeast CENP-T homologue Cnn1 binds to Spc24/25 (Schleiffer *et al*, 2012) and the crystal structure of the Cnn1–Spc24/25 complex is similar to that of the chicken CENP-T–Spc24/25 complex (Stefan Westermann, personal communication), although with some intriguing differences in orientation and phospho-regulation.

The phosphorylated CENP-T N-terminal region binds to the Ndc80 complex using unique structural features

Our structural studies indicate that phosphorylation of several residues in the CENP-T N-terminal region is required for its interaction with the Ndc80 complex, but that these sites are not directly involved in the interaction with Spc24/25. Instead, the phospho-mimetic T72D CENP-T residue forms a salt bridge with R74 to allow the downstream hydrophobic residues to interact with Spc24/25. This is in contrast with a canonical phospho-peptide-protein interaction such as phospho-S/T binding for 14-3-3 family proteins (Yaffe and Elia, 2001; Yaffe and Smerdon, 2001). Negatively charged phospho-peptides bind to a positively charged pocket in 14-3-3 proteins with the phosphorylated residues directly involved in the interaction. This interaction mode has provided a major model for phospho-dependent protein interactions (Yaffe and Elia, 2001). The binding of phosphorylated CENP-T with the Spc24/25 complex represents a distinct model for generating phospho-dependent protein interactions. The binding mode of phosphorylated CENP-T is similar to that of RNA polymerase II recognition by 3′-RNA processing factors in which phosphorylation of RNA polymerase II is not directly involved in recognition of 3′-RNA processing factors, but stabilizes the β-turn with an additional hydrogen bond (Meinhart and Cramer, 2004).

In addition to the phospho-dependent interaction of CENP-T with Spc25, we also found a second hydrophobic-interaction surface between CENP-T and Spc24 that involves the L68 residue of CENP-T. CENP-T L68R mutants failed to interact with the Spc24/25 complex even in the phospho-mimetic form (Figure 4). This indicates that CENP-T has multiple hydrophobic-interaction sites for the Spc24/25 complex. Although CENP-T phosphorylation strongly enhances binding to the Spc24/25 complex, the hydrophobic interactions form the basis for the CENP-T–Spc24/25 association.

Structure predictions suggest that the CENP-T N-terminal region is largely unstructured (Supplementary Figure S3; Suzuki *et al*, 2011). In recent years, many proteins have been discovered that are unstructured alone, but form defined structures upon binding their biological targets (Dyson and Wright, 2005). For example, the N-terminal histone tails are unstructured alone, but when modifications such as methylation occur in this region, the modified tail is able to bind to target proteins such as HP1 resulting in the formation of a discrete structure. Moses *et al* (2007) proposed that CDK target sites are frequently clustered in such unstructured regions. Indeed, we have found that

CDK target sites are clustered in the unstructured region of CENP-T (Supplementary Figure S3). Once the CENP-T N-terminal region is phosphorylated, CENP-T binds to the Spc24/25 complex and forms a defined three-dimensional structure. The T-P-R residues (72–74) that are required for CENP-T phosphorylation and the downstream hydrophobic residues are well conserved. However, the T72 residue is absent in some fungi including *S. cerevisiae* Cnn1/CENP-T (Bock *et al*, 2012; Schleiffer *et al*, 2012; Supplementary Figure S3). Instead, the phosphorylated threonine residue is replaced with a glutamate in budding yeast. Pearlman *et al* (2011) demonstrated that some phosphorylation sites in proteins such as DNA-topoII, enolase, and C-Raf are changed to negatively charged amino acids (D/E) during evolution, thus mimicking the presence of a constitutively phosphorylated residue. Although budding yeast Cnn1/CENP-T does not appear to use a similar binding mode (Stefan Westermann, personal communication), the glutamate residue may form an unidentified salt bridge with positively charged residues to generate a non-regulated interaction between CENP-T/Cnn1 and the Ndc80 complex. The T-P-R sequence and the downstream hydrophobic residues found in CENP-T efficiently enhance the hydrophobic interaction between CENP-T and Spc24/25, providing a unique way to facilitate protein–protein interactions.

RWD domains serve as interaction modules at kinetochores

The globular region of the Spc24/25 complex contains an 'RWD' domain found in RING finger proteins, WD-repeat containing proteins, and DEXD-like helicases, which is composed of two similar folded $\alpha+\beta$ sandwiches (Schmitzberger and Harrison, 2012). Recently, the structure of the yeast Ctf19-Mcm21 complex, which corresponds to the vertebrate CENP-P-O complex, was determined and found to also contain an RWD domain (Schmitzberger and Harrison, 2012). An RWD domain is also found in the kinetochore protein Csm1 (Corbett *et al*, 2010). As at least five different kinetochore proteins contain this RWD domain, Schmitzberger and Harrison (2012) proposed that the RWD domain is an important interaction module to assemble the kinetochore. However, it was unclear how other kinetochore proteins interact with this domain. The structure of the CENP-T–Spc24/25 complex provides evidence that the RWD domain serves as an interaction module for kinetochore assembly. RWD domains are also found in Gcn2, ubiquitin ligase, and FANCL (Schmitzberger and Harrison, 2012). Based on the work described here for the CENP-T–Spc24/25 interaction, hydrophobic residues in RWD domains make important contributions to protein–protein interactions, and phosphorylation of RWD binding partners may facilitate additional hydrophobic interactions.

CENP-T is structural hub for formation of functional kinetochores

Previous biochemical studies revealed that the Ndc80 complex associates with the Mis12 complex, which in turn interacts with the inner kinetochore protein CENP-C (Cheeseman *et al*, 2004; Obuse *et al*, 2004; Gascoigne *et al*, 2011; Przewloka *et al*, 2011; Screpanti *et al*, 2011). Petrovic *et al* (2010) demonstrated that the Nsl1 subunit of the Mis12 complex binds to tightly to Spc24/25. We previously found that, although the localization of the Ndc80 complex to kinetochores is reduced in Mis12- or CENP-C-deficient cells (Kline *et al*, 2006; Kwon *et al*, 2007; Gascoigne *et al*, 2011), Ndc80 localization was also reduced in CENP-H- or CENP-T-deficient cells (Okada *et al*, 2006; Hori *et al*, 2008; Gascoigne *et al*, 2011). As CENP-C and CENP-T localization is independent (Hori *et al*, 2008; Gascoigne *et al*, 2011) and we demonstrated that the binding of CENP-T and the Mis12 complex to Spc24/25 was mutually exclusive in this study, we propose that there are two parallel pathways for outer kinetochore assembly. Such parallel pathways have also been proposed from the study of the yeast CENP-T homologue Cnn1 (Stefan Westerman, personal communication). It is important to define how these pathways are organized to recruit the Ndc80 complex to kinetochores. It is possible that the Ndc80 complex shows temporally regulated binding such that it interacts with the Mis12 complex and CENP-T at distinct times in mitosis. However, CENP-T is phosphorylated throughout mitosis (Gascoigne *et al*, 2011) and the interaction of the Mis12 complex with the Ndc80 complex also occurs during mitosis. Therefore, in vertebrates it is likely that these two pathways act simultaneously. *C. elegans* and *D. melanogaster* lack visible CENP-T homologues and the analyses that have been done indicate that compromising the Mis12 pathway results in a kinetochore null phenotype. Therefore, it may be sufficient to have a single Ndc80 recruitment pathway to assemble the chromosome-segregation machinery. The two pathways that are present in vertebrates and fungi may act redundantly to strengthen the connection between the inner and outer kinetochore, or may recruit functionally distinct populations of the Ndc80 complex.

Materials and methods

Protein preparation and size-exclusion chromatography

Chicken and human Spc24 and Spc25 globular domains were cloned into pRSFduet co-expression vector. 6 × his-TEV-Spc25 (chicken 132–234 aa, human 70–224 aa, and human 129–224 aa) and StrepII-TEV-Spc24 (chicken 125–195 aa, human 57–197 aa, and human 131–197 aa) were expressed in BL21 (DE3) Star-pRARE2LysS by the addition of 0.2 mM IPTG for 16 h at 16°C. The Spc24/25 complex was purified using Ni-Sepharose, TEV cleavage and a Superdex 200 column. Chicken CENP-Ts (2–98 aa, 63–98 aa, or 2–50 aa) and human CENP-Ts (76–106 aa or 2–32 aa) were cloned into pMal-TEV-CENPT-6 × His vector to prepare MBP-fused proteins. MBP-CENP-Ts were expressed in same condition as the Spc24/25 complex. MBP-CENP-Ts were purified by Ni-Sepharose and Superdex 200 column. For crystallography, the CENP-T–Spc24/25 complex was co-expressed in BL21(DE3)Star-pRARE2Lys by co-transforming pRSFduet-Spc24-Spc25 and pMal-6 × His-TEV-CENPT vectors. The CENP-T–Spc24/25 complex was purified by Ni-Sepharose, Superdex 200 column, TEV cleavage and Superdex 200 column.

For expression of the human 6 × His-Mis12-KNL1$^{2106–2316}$ complex, 6 × His-Mis12 complex (Kline *et al*, 2006) was co-expressed with untagged KNL1$^{2106–2316}$ and purified as described previously. Also see Petrovic *et al* (2010). CENP-T-6 × His (aa 1-375) wild-type and T85D (created by site-directed mutagenesis using QuikChange (Agilent Technologies)) constructs were expressed under the same conditions as the 6 × His-Mis12. The Ndc80^{Bonsai} complex was expressed as described previously (Ciferri *et al*, 2008). The Ndc80^{Bonsai} I149A_L154A mutant was generated by site-directed mutagenesis using QuikChange (Agilent Technologies). Proteins were purified using Glutathione agarose (Sigma) or Ni-NTA agarose (QIAGEN) according to manufacturer's guidelines and then exchanged into 50 mM Tris (pH 7.6), 200 mM NaCl, 1 mM DTT, followed by size-exclusion chromatography.

Analytical size-exclusion chromatography experiments were performed on a calibrated Superose 6 10/300 column in the presence of 50 mM Tris (pH 7.6), 200 mM NaCl, 1 mM DTT at a flow rate of 0.3 ml/min. Elution of proteins was monitored at $A_{280\ nm}$. To detect complex formation, proteins were mixed together in a volume of 500 μl at final concentrations of 4 μM each for pairwise mixing experiments and 1, 5, and 25 μM in competition experiments for KNL1^{CT}/Mis12, Ndc80^{Bonsai}, and hsCENP-T-MBP, respectively. Protein mixtures were incubated on ice for 30 min before conducting the chromatography. Fractions were collected and analysed by SDS–PAGE and Coomassie staining.

Crystallization and structural determination of the Spc24/25 complex and CENP-T–Spc24/25 complex

The chicken Spc24/25 complex was crystallized by mixing equal amounts of the protein solution (10 mg/ml) and MORPHEUS crystallization screening kit F1 solution (Molecular Dimensions; Gorrec, 2009), which contained a mixture of 0.12 M Monosaccharides, 0.1 M MES-Imidazol pH 6.5, and 30% PEG20K/P550MME. Crystals were harvested in crystallization solution and were flash frozen under nitrogen stream. X-ray diffraction data were collected at BL44XU in the SPring8 synchrotron facility. Diffraction data were processed by HKL2000 package. Structure was determined by molecular replacement using Phenix package (Adams *et al*, 2010). The Spc24/25 coordinate from the human Ndc80^{Bonsai} complex (PDB ID = 2VE7) was used as a search model. Model was refined using iterative modelling and refinement. The final model contains Spc24 (136–195 aa), Spc25 (131–233 aa), and 251 water molecules.

The chicken CENP-T–Spc24/25 complex was crystallized by mixing equal amount of protein solution (10 mg/ml) and PACT premier F10 solution (Molecular Dimensions; Newman *et al*, 2005) which contained a mixture of 0.02 M Na/K phosphate, 0.1 M Bis Tris propane pH 6.5 and 20% PEG 3350. Crystals were harvested in crystallization solution and were cryoprotected by the addition of 20% glycerol in final concentration. X-ray diffraction data were collected at BL38B1 in the SPring8 synchrotron facility. Diffraction data were processed by HKL2000 package. Structure was determined by molecular replacement using Phenix package. The chicken Spc24/25 complex was used as a search model and refined iteratively. The final model contains CENP-T (63–93 aa), Spc24 (134–195 aa), Spc25 (134–232 aa) and 357 water molecules. Figures were prepared using PyMOL package (DeLano Scientific LLC).

Cell culture

DT40 cells were cultured as described previously (Okada *et al*, 2006). Spc25-deficient cells were created using standard methods.

Immunofluorescence and light microscopy

Chicken DT40 cells were cultured and transfected as described previously (Okada *et al*, 2006). Immunofluorescent staining of DT40 cells was performed as described previously using anti-CENP-T, anti-Mis12, or anti-Ndc80 antibodies (Kline *et al*, 2006; Okada *et al*, 2006; Hori *et al*, 2008). Immunofluorescence images were collected with a cooled EM CCD camera (QuantEM, Roper Scientific) mounted on an Olympus IX71 inverted microscope with a × 100 objective together with a filter wheel and a DSU confocal unit. 15-25 Z-sections were acquired at 0.3 μm steps. Fluorescence intensity measurements were conducted using MetaMorph software (Molecular Devices). Kinetochore fluorescence intensities were determined by measuring the integrated fluorescence intensity within a 6 × 6 pixel square positioned over a single kinetochore and subtracting the background intensity of a 6 × 6 pixel square positioned in a region of cytoplasm lacking kinetochores. Maximal projected images were used for these measurements.

Isothermal titration calorimetry

For interaction between CENP-T fusion protein, CENP-T peptides, and the Spc24/25 complex, proteins were dialysed in 10 mM Hepes pH 7.4, 500 mM NaCl and 1 mM DTT. CENP-T was diluted to 100 μM and titrated into 10 μM of Spc24-25. For interaction between human CENP-T, the Mis12 complex and the Spc24/25 complex, proteins were dialysed in 10 mM Hepes pH 7.4, 150 mM NaCl, and 1 mM TCEP. The Spc24/25 complex was diluted to 100 μM and titrated into 10 μM of the Mis12 complex. CENP-T was diluted to 100 μM and titrated into 10 μM of the Spc24/25 complex. Interaction between CENP-T, the Mis12 complex, and the Spc24/25 complex was measured by AutoiTC200 (GE Healthcare) and the data were analysed with Origin 7 software (MicroCal).

Composition gradient-multi angle light scattering

CG-MALS between MBP-CENP-T and the Spc24/25 complex was measured by CalypsoII system (Wyatt Technology Corp.). In all, 10 μM of each solution was mixed in 10 different composition gradients and their static light scattering was measured by DAWN-HELIOS system. Optilab differential refractometer and UV absorption detector were used to measure the protein concentration. Data were analysed by CalypsoII system software.

Accession numbers

The Protein Data Bank (PDB) IDs of the chicken the Spc24/25 complex and the CENP-T-Spc24/25 complex are 3VZ9 and 3VZA, respectively.

Supplementary data

Supplementary data are available at *The EMBO Journal* Online (http://www.embojournal.org).

Acknowledgements

We are grateful to M Takahashi, K Suzuki, K Nakaguchi, and K Kita for technical assistance. We thank M Ariyoshi and T Oyama for help with diffraction data collection. The synchrotron radiation experiments were performed at the BL38B1 and BL44XU of SPring-8 with the approval of the Japan Synchrotron Radiation Research Institute (JASRI) (Proposal No. 2010B1059, 2010B1060, and 2011A1211). We also thank T Nakagawa for help in the measurement of CG-MALS and K Maenaka, T Saito and F Oosaka for help in the measurement of ITC. This work was supported by Grants-in-Aid for Scientific Research from the Ministry of Education, Culture, Sports, Science and Technology (MEXT) of Japan and the Cabinet Office, Government of Japan through its 'Funding Program for Next Generation World-Leading Researchers' to TF, grants from the Searle Scholars Program and the NIH/National Institute of General Medical Sciences (GM088313) to IMC, and a National Science Foundation graduate research fellowship to FR. TN is supported by The International Human Frontier Science Program Organization grant and by Grants-in-Aid for Scientific Research from MEXT.

Author contributions: TN designed and performed structural and biochemical experiments for chicken and human recombinant protein complexes. TH and TF performed cell biological experiments with DT40 cells. FR and IMC performed biochemical experiments with human recombinant proteins and cell biological studies with human cells. KT analysed CENP-T sequences in various species. TN, IMC, and TF wrote the manuscript.

Conflict of interest

The authors declare that they have no conflict of interest.

References

Adams PD, Afonine PV, Bunkóczi G, Chen VB, Davis IW, Echools N, Headd JJ, Hung L-W, Kapral GJ, Grosse-Kunstleve RW, McCoy AJ, Moriarty NW, Oeffner R, Read RJ, Richardson DC, Richardson JS, Terwilliger TC, Zwart PH (2010) PHENIX: a comprehensive Python-based system for macromolecular structure solution. *Acta Crystallogr D Biol Crystallogr* **D66:** 213–221

Alushin GM, Ramey VH, Pasqualato S, Ball DA, Grigorieff N, Musacchio A, Nogales E (2010) The Ndc80 kinetochore complex forms oligomeric arrays along microtubules. *Nature* **467:** 805–810

Amano M, Suzuki A, Hori T, Backer C, Okawa K, Cheeseman IM, Fukagawa T (2009) The CENP-S complex is essential for the stable assembly of outer kinetochore structure. *J Cell Biol* **186:** 173–182

Bock LJ, Pagliuca C, Kobayashi N, Grove RA, Oku Y, Shrestha K, Alfieri C, Golfieri C, Oldani A, Dal Maschio M, Bermejo R, Hazbun TR, Tanaka TU, De Wulf P (2012) Cnn1 inhibits the interactions between the KMN complexes of the yeast kinetochore. *Nat Cell Biol* **14:** 614–624

Cheeseman IM, Chappie JS, Wilson-Kubalek EM, Desai A (2006) The conserved KMN network constitutes the core microtubule-binding site of the kinetochore. *Cell* **127:** 983–997

Cheeseman IM, Desai A (2008) Molecular architecture of the kinetochore-microtubule interface. *Nat Rev Mol Cell Biol* **9:** 33–46

Cheeseman IM, Hori T, Fukagawa T, Desai A (2008) KNL1 and the CENP-H/I/K complex coordinately direct kinetochore assembly in vertebrates. *Mol Biol Cell* **19:** 587–594

Cheeseman IM, Niessen S, Anderson S, Hyndman F, Yates III JR, Oegema K, Desai A (2004) A conserved protein network controls assembly of the outer kinetochore and its ability to sustain tension. *Genes Dev* **18:** 2255–2268

Ciferri C, Pasqualato S, Screpanti E, Varetti G, Santaguida S, Dos Reis G, Maiolica A, Polka J, De Luca JG, De Wulf P, Salek M, Rappsilber J, Moores CA, Salmon ED, Musacchio A (2008) Implications for kinetochore-microtubule attachment from the structure of an engineered Ndc80 complex. *Cell* **133:** 427–439

Corbett KD, Yip CK, Ee LS, Walz T, Amon A, Harrison SC (2010) The monopolin complex crosslinks kinetochore components to regulate chromosome-microtubule attachments. *Cell* **142:** 556–567

DeLuca JG, Gall WE, Ciferri C, Cimini D, Musacchio A, Salmon ED (2006) Kinetochore microtubule dynamics and attachment stability are regulated by Hec1. *Cell* **127:** 969–982

DeLuca JG, Moree B, Hickey JM, Kilmartin JV, Salmon ED (2002) hNuf2 inhibition blocks stable kinetochore-microtubule attachment and induces mitotic cell death in HeLa cells. *J Cell Biol* **159:** 549–555

DeLuca JG, Musacchio A (2012) Structural organization of the kinetochore-microtubule interface. *Curr Opin Cell Biol* **24:** 48–56

Dyson HJ, Wright PE (2005) Intrinsically unstructured proteins and their functions. *Nature Rev Mol Cell Biol* **6:** 197–208

Gascoigne KE, Takeuchi K, Suzuki A, Hori T, Fukagawa T, Cheeseman IM (2011) Induced ectopic kinetochore assembly bypasses the requirement for CENP-A nucleosomes. *Cell* **145:** 410–422

Gorrec F (2009) The MORPHEUS protein crystallization screen. *J Appl Cryst* **42:** 1035–1042

Hori T, Amano M, Suzuki A, Backer CB, Welburn JP, Dong Y, McEwen BF, Shang YH, Suzuki E, Okawa K, Cheeseman IM, Fukagawa T (2008) CCAN makes multiple contacts with centromeric DNA to provide distinct pathways to the outer kinetochore. *Cell* **135:** 1039–1052

Hori T, Haraguchi T, Hiraoka Y, Kimura H, Fukagawa T (2003) Dynamic behavior of Nuf2-Hec1 complex that localizes to the centrosome and centromere and is essential for mitotic progression in vertebrate cells. *J Cell Sci* **116:** 3347–3362

Kiyomitsu T, Obuse C, Yanagida M (2007) Human Blinkin/AF15q14 is required for chromosome alignment and the mitotic checkpoint through direct interaction with Bub1 and BubR1. *Dev Cell* **13:** 663–676

Kline SL, Cheeseman IM, Hori T, Fukagawa T, Desai A (2006) The human Mis12 complex is required for kinetochore assembly and proper chromosome segregation. *J Cell Biol* **173:** 9–17

Kwon MS, Hori T, Okada M, Fukagawa T (2007) CENP-C is involved in chromosome segregation, mitotic checkpoint function, and kinetochore assembly. *Mol Biol Cell* **18:** 2155–2168

Liu ST, Rattner JB, Jablonski SA, Yen TJ (2006) Mapping the assembly pathways that specify formation of the trilaminar kinetochore plates in human cells. *J Cell Biol* **175:** 41–53

Martin-Lluesma S, Stucke VM, Nigg EA (2002) Role of Hec1 in spindle checkpoint signaling and kinetochore recruitment of Mad1/Mad2. *Science* **297:** 2267–2270

Maskell DP, Hu XW, Singleton MR (2010) Molecular architecture and assembly of the yeast kinetochore MIND complex. *J Cell Biol* **190:** 823–834

McCleland ML, Gardner RD, Kallio MJ, Daum JR, Gorbsky GJ, Burke DJ, Stukenberg PT (2003) The highly conserved Ndc80 complex is required for kinetochore assembly, chromosome congression, and spindle checkpoint activity. *Genes Dev* **17:** 101–114

McCleland ML, Kallio MJ, Barrett-Wilt GA, Kestner CA, Shabanowitz J, Hunt DF, Gorbsky GJ, Stukenberg PT (2004) The vertebrate Ndc80 complex contains Spc24 and Spc25 homologs, which are required to establish and maintain kinetochore-microtubule attachment. *Curr Biol* **14:** 131–137

McIntosh JR, Grishchuk EL, Morphew MK, Efremov AK, Zhudenkov K, Volkov VA, Cheeseman IM, Desai A, Mastronarde DN, Ataullakhanov FI (2008) Fibrils connect microtubule tips with kinetochores: a mechanism to couple tubulin dynamics to chromosome motion. *Cell* **135:** 322–333

Meinhart A, Cramer P (2004) Recognition of RNA polymerase II carboxy-terminal domain by 3′-RNA-processing factors. *Nature* **430:** 223–226

Moses AM, Hériché JK, Durbin R (2007) Clustering of phosphorylation site recognition motifs can be exploited to predict the targets of cyclin-dependent kinase. *Genome Biol* **8:** R23

Newman J, Egan D, Walter TS, Meged R, Berry I, Ben Jelloul M, Sussman JL, Stuart DI, Perrakis A (2005) Towards rationalization of crystallization screening for small- to medium-sized academic laboratories: the PACT/JCSG+ strategy. *Acta Crystallogr D Biol Crystallogr* **61:** 1426–1431

Nishimura K, Fukagawa T, Takisawa H, Kakimoto T, Kanemaki M (2009) An auxin-based degron system for the rapid depletion of proteins in nonplant cells. *Nat Methods* **6:** 917–922

Nishino T, Takeuchi K, Gascoigne KE, Suzuki A, Hori T, Oyama T, Morikawa K, Cheeseman IM, Fukagawa T (2012) CENP-T-W-S-X forms a unique centromeric chromatin structure with a histone-like fold. *Cell* **148:** 487–501

Obuse C, Iwasaki O, Kiyomitsu T, Goshima G, Toyoda Y, Yanagida M (2004) A conserved Mis12 centromere complex is linked to heterochromatic HP1 and outer kinetochore protein Zwint-1. *Nat Cell Biol* **6:** 1135–1141

Okada M, Cheeseman IM, Hori T, Okawa K, McLeod IX, Yates III JR, Desai A, Fukagawa T (2006) The CENP-H-I complex is required for the efficient incorporation of newly synthesized CENP-A into centromeres. *Nat Cell Biol* **8:** 446–457

Pearlman SM, Serber Z, Ferrell Jr JE (2011) A mechanism for the evolution of phosphorylation sites. *Cell* **147:** 934–946

Perpelescu M, Fukagawa T (2011) The ABCs of CENPs. *Chromosoma* **120:** 425–446

Petrovic A, Pasqualato S, Dube P, Krenn V, Santaguida S, Cittaro D, Monzani S, Massimiliano L, Keller J, Tarricone A, Maiolica A, Stark H, Musacchio A (2010) The MIS12 complex is a protein interaction hub for outer kinetochore assembly. *J Cell Biol* **190:** 835–852

Powers AF, Franck AD, Gestaut DR, Cooper J, Gracyzk B, Wei RR, Wordeman L, Davis TN, Asbury CL (2009) The Ndc80 kinetochore complex forms load-bearing attachments to dynamic microtubule tips via biased diffusion. *Cell* **136:** 865–875

Przewloka MR, Venkei Z, Bolanos-Garcia VM, Debski J, Dadlez M, Glover DM (2011) CENP-C is a structural platform for kinetochore assembly. *Curr Biol* **21:** 399–405

Santaguida S, Musacchio A (2009) The life and miracles of kinetochores. *EMBO J* **28:** 2511–2531

Schleiffer A, Maier M, Litos G, Lampert F, Hornung P, Mechtler K, Westermann S (2012) CENP-T proteins are conserved centromere receptors of the Ndc80 complex. *Nat Cell Biol* **14:** 604–613

Schmitzberger F, Harrison SC (2012) RWD domain: a recurring module in kinetochore architecture shown by a Ctf19-Mcm21 complex structure. *EMBO Rep* **13:** 216–222

Screpanti E, De Antoni A, Alushin GM, Petrovic A, Melis T, Nogales E, Musacchio A (2011) Direct binding of Cenp-C to the Mis12 complex joins the inner and outer kinetochore. *Curr Biol* **21:** 391–398

Suzuki A, Hori T, Nishino T, Usukura J, Miyagi A, Morikawa K, Fukagawa T (2011) Spindle microtubules generate tension-dependent changes in the distribution of inner kinetochore proteins. *J Cell Biol* **193:** 125–140

Wei RR, Al-Bassam J, Harrison SC (2007) The Ndc80/HEC1 complex is a contact point for kinetochore-microtubule attachment. *Nat Struct Mol Biol* **14:** 54–59

Wei RR, Schnell JR, Larsen NA, Sorger PK, Chou JJ, Harrison SC (2006) Structure of a central component of the yeast kinetochore: the Spc24p/Spc25p globular domain. *Structure* **14:** 1003–1009

Wilson-Kubalek EM, Cheeseman IM, Yoshioka C, Desai A, Milligan RA (2008) Orientation and structure of the Ndc80 complex on the microtubule lattice. *J Cell Biol* **182:** 1055–1061

Yaffe MB, Elia AE (2001) Phosphoserine/threonine-binding domains. *Curr Opin Cell Biol* **13:** 131–138

Yaffe MB, Smerdon SJ (2001) PhosphoSerine/threonine binding domains: you can't pSERious? *Structure* **9:** R33–R38

